ORIGINAL ARTICLE

MicrobiologyOpen Open Access WILEY

Dynamic changes occur in the DNA gut virome of female cynomolgus macaques during aging

Xunmin Tan[1,2] | Tingjia Chai[2,3] | Jiajia Duan[2,4] | Jing Wu[2,4] | Hanping Zhang[1,2] | Yifan Li[1,2] | Yu Huang[1,2] | Xi Hu[1] | Peng Zheng[1,2] | Jinlin Song[5,6,7] | Ping Ji[5,6] | Xin Jin[6,8] | Hongmei Zhang[5,6] | Peng Xie[1,2] 🄳

[1]Department of Neurology, The First Affiliated Hospital of Chongqing Medical University, Chongqing, China

[2]NHC Key Laboratory of Diagnosis and Treatment on Brain Functional Diseases, Chongqing Medical University, Chongqing, China

[3]State Key Laboratory of Ultrasound in Medicine and Engineering, College of Biomedical Engineering, Chongqing Medical University, Chongqing, China

[4]The M.O.E. Key Laboratory of Laboratory Medical Diagnostics, The College of Laboratory Medicine, Chongqing Medical University, Chongqing, China

[5]College of Stomatology, Chongqing Medical University, Chongqing, China

[6]Chongqing Key Laboratory for Oral Diseases and Biomedical Sciences, Chongqing, China

[7]Chongqing Municipal Key Laboratory of Oral Biomedical Engineering of Higher Education, Chongqing, China

[8]Key Laboratory of Psychoseomadsy, Stomatological Hospital of Chongqing Medical University, Chongqing, China

Correspondence
Peng Xie, Department of Neurology, The First Affiliated Hospital of Chongqing Medical University, Chongqing, China.
Email: xiepeng@cqmu.edu.cn

Abstract

Aging is a critical factor affecting physical health and disease in mammals. Emerging evidence indicates that aging may affect the gut bacteriome in cynomolgus macaques, but little is known about whether or how the gut virome changes with age. Here, we compared the DNA gut viral composition of 16 female cynomolgus monkeys (*Macaca fascicularis*) at three life stages (young, adult, and old) using the shotgun metagenome sequencing method. We found that the DNA gut virome from these monkeys differed substantially among the three groups. The gut viruses were dominated by bacteriophages, the most abundant of which was the *Caudovirales* order (i.e., *Siphoviridae*, *Myoviridae*, and *Podoviridae* families). Additionally, the co-occurrence analysis revealed that the age-related bacteriophages were correlated in an extensive and complex manner with the main intestinal bacteria (i.e., *Firmicutes*, *Bacteroidetes*, *Proteobacteria*, and *Actinobacteria* phyla). Furthermore, the age-related DNA gut viral functions were enriched for genetic information processing, nucleotide, and folate metabolism. Our gut virome analysis provides new insight into how aging influences the gut virome of non-human primates.

KEYWORDS
aging, bacteriophages, cynomolgus macaques, DNA gut virome, shotgun metagenome sequencing

---

Xunmin Tan and Tingjia Chai contributed equally.

1 | INTRODUCTION

Aging often negatively impacts the vitality and health of human beings. For example, previous studies have shown that aging is implicated in the development of atherosclerosis (Wang & Bennett, 2012), Alzheimer's disease (Qiu et al., 2009), and innate immune dysregulation (Shaw et al., 2013). Accompanied by a broad influence on the general physiology of the gastrointestinal tract, the aging process also inevitably affects gut microbes in human beings (Biagi et al., 2010) or non-human primates (Duan et al., 2019). The gut microbiome is composed of bacteria, eukaryotic viruses, bacterial viruses (bacteriophages), fungi, and archaea. Numerous studies have reported that gut microbial homeostasis plays an essential part in maintaining human health (Gentile & Weir, 2018; Lynch & Pedersen, 2016). Disturbance of gut microbiota is also implicated in a wide range of human diseases such as cancer (Flemer et al., 2017; Matson et al., 2018), obesity (Sharma et al., 2018), and neuropsychiatric conditions (Sampson et al., 2016; Sharon et al., 2019). Some studies have focused on how aging modulates the gut bacteriome. Our previous research, for example, found that the gut bacteriome changed significantly with age, as demonstrated by enriched *Veillonellaceae*, *Coriobacteriaceae*, and *Succinivibrionaceae*, and depleted *Ruminococcaceae* and *Rikenellaceae* in old monkeys relative to their young counterparts (Duan et al., 2019). However, it remains unknown whether and how aging shapes the gut virome.

Recently, some studies have shown that the gut virome plays a crucial role in maintaining human health and that chronic viral infections can confer symbiotic protection from bacterial infection (Barton et al., 2007), suggesting that not all viruses are harmful to their hosts (Virgin, 2014). However, investigations on the human gut virome are still in their infancy, and a great host of human viruses await identification. To date, two studies have characterized the human intestinal virome and bacteriome in infant and adult monozygotic twins. Lim et al. (Lim et al., 2015) investigated the dynamic changes occurring in the gut virome and bacteriome at six time points from birth to 2 years of age in infant monozygotic twins. Moreno-Gallego et al. (2019) explored the interactions occurring between the gut virome and bacteriome in adult monozygotic twins. Both studies highlight the dynamic nature of the human gut virome and the association between gut viruses and microbes in infant and adult monozygotic twins during a relatively short period, but information on the human gut virome from youth to old age is eagerly awaited. The human gut virome is complex, and its composition is relatively unstable because of the numerous confounding factors that can affect it (e.g., diet, antibiotics use, and environmental and geographical factors; Górska et al., 2018; Minot et al., 2011; Rampelli et al., 2017). Instead, as non-human primates, cynomolgus macaques are not only closely related to human beings in genetics but unlike humans, they are more likely to keep their diet, nutritional status, health condition, and geographical location consistent.

To elucidate the impact of aging on the gut virome in non-human primates, we investigated the composition and function of the gut virome from five young (2–4 years), six adult (5–15 years), and five old (17–20 years) female cynomolgus macaques using shotgun metagenome sequencing. We found that the DNA gut virome in the monkeys was dominated by phages, most of which belonged to the *Caudovirales* order, including *Myoviridae*, *Siphoviridae*, and *Podoviridae* families. Moreover, a complex and diverse relationship was identified between age-related bacteriophages and bacteria. Collectively, our findings augment the current understanding of the relationship between the gut virome and aging in non-human primates.

2 | MATERIALS AND METHODS

2.1 | Study subject selection and fecal sample collections

All the cynomolgus monkeys (crab-eating macaques, *Macaca fascicularis*) used in the experiments were provided by Zhongke Experimental Animal Co., Ltd. The animals lived under the following standard conditions: 22 ± 1°C temperature, 50 ± 5% relative humidity, and 12-h light/12-h dark cycle with lights on at 07:00 (Zheng et al., 2020). Stool samples were obtained from 5 young (2–4 years), 6 adult (5–15 years), and 5 old (17–20 years) female cynomolgus macaques (Appt et al., 2010; Drevon-Gaillot et al., 2006; Wang et al., 2020), all of which had the same living conditions, daily diet and health qualities (Xu et al., 2012). All the stool samples from the selected monkeys were collected with a sterile device without any medium and stored at −80°C until subsequent processing.

2.2 | Shotgun metagenome sequencing and taxonomic assignments

The shotgun metagenome sequencing protocol was based on our previous published work (Yang et al., 2020; Zheng et al., 2020). Briefly, microbial DNA was extracted from the fecal samples using the E.Z.N.A® DNA kit (Omega Bio-Tek) according to the manufacturer's instructions. The concentration and purity of the DNA extracted from the stool samples were qualified and assessed by a NanoDrop 2000 spectrophotometer (Thermo Fisher Scientific) for the construction of the metagenome shotgun sequencing libraries. Each library was sequenced on the Illumina HiSeq 4000 platform (Illumina Inc.) at Majorbio Bio-Pharm Technology Co., Ltd. using the HiSeq 3000/4000 PE Cluster Kit and the HiSeq 3000/4000 SBS Kit according to the manufacturer's instructions (www.illumina.com). Host reads were determined and removed according to the sequence alignments with the Bayesian model averaging (Zheng et al., 2020). Low-quality sequences were discarded using Sickle (https://github.com/najoshi/sickle). The remaining high-quality sequences were assembled using SOAPaligner (Li et al., 2008) to evaluate the gene abundance in each sample.

To cluster the viral sequences, the representative sequences of a nonredundant gene catalog were aligned against the National

Center for Biotechnology Information (NCBI) NR database using an e-value cutoff of 1e-5 with BLASTP (Version 2.2.28+) for taxonomic annotations. Kyoto encyclopedia of genes and genomes (KEGG) annotation was conducted using BLASTP (Version 2.2.28+) against the KEGG database (Xie et al., 2011) using an e-value cutoff of 1e-5. The unit of gene abundance was unified using reads per kilobase million.

2.3 | Metagenomic analysis of fecal samples

Based on the taxonomy annotation for viruses, α-diversity, a measure of viral community richness (Chao and Ace index) and diversity (Shannon and Invsimpson index) at the species level, was assessed and visualized using the vegan and fossil packages in R, respectively. β-diversity was assessed based on Abund–Jaccard distance and visualized by principal coordinate analysis (PCoA). ANOSIM (analysis of similarities) was performed to identify differences in β-diversity among the three age groups. The key viral and bacterial taxa and the KEGG categories responsible for discrimination among the three age groups were identified using linear discriminant analysis effective size, LEfSe (Segata et al., 2011). Only linear discriminant analysis (LDA) values >2.0 and p values <0.05 were considered to represent significantly enriched taxa.

2.4 | Statistical analysis

Statistical analyses were carried out using SPSS version 21.0 (SPSS), and plots were generated from R packages (pheatmap, ggplot2), GraphPad Prism (version 8.0), and Cytoscape (version 3.7.2). Continuous variables such as age were analyzed using ANOVA followed by LSD multiple comparison tests. We applied the non-parametric factorial Kruskal–Wallis test followed by Dunn's multiple comparison tests to compare the three groups in cases of heteroscedasticity or non-normally distributed variables. Correlations between age-related bacteriophages and bacteria were tested by Spearman's correlation analysis. Statistical significance was set at <0.05.

3 | RESULTS

3.1 | Shotgun metagenomes of cynomolgus stool samples in DNA virus domain

We obtained fecal samples from 16 female cynomolgus macaques between the ages of 2 and 20. The detailed characteristics of all the study subjects were listed in our previously published report (Duan et al., 2019). On average, we obtained 101,290,630 ± 7,898,542 (mean ±s.d.) paired reads per sample. After quality control, 100,140,304 ± 7,837,876 paired reads per sample were used to de novo assemble the microbial contigs. We identified 18,773,882

predicted genes from the filtered sequence data, from which a non-redundant gene set containing 9317 genes was assigned to the viral microbiome which comprised only the DNA gut virome and used for subsequent analyses.

3.2 | Similar α-diversity of the gut DNA virome among the three age groups

Initially, a downward trend in α-diversity was detected for the viral richness (Chao and Ace index) at increased age, but no significant difference was observed (one-way ANOVA, all p values >0.05; Figure 1a). Furthermore, our pan analysis illustrated that the rate at which viruses accumulated declined with age, suggesting that the downward trend in viral richness was not likely attributable to different sample sizes (Figure 1b). Similarly, we found that the gut viral richness was highest in the young and gradually decreased with age, although no statistical difference was detected at the quantified levels (one-way ANOVA, p = 0.206; Figure 1c). Intriguingly, viral diversity (Invsimpson and Shannon index) decreased in the adult age-group versus the young, a finding reversed in the oldest age-group (one-way ANOVA, all p values >0.05; Figure 1a).

3.3 | The global composition of gut DNA virome shifted with age

We compared β-diversity at the species level using the Abund–Jaccard distance metric. PCoA of the gut DNA virome revealed clear segregation among the young, adult, and old female cynomolgus macaques (ANOSIM, r = 0.153, p = 0.024; Figure 1d). This suggested that aging contributed to the variation in the global phenotypes of gut DNA virome in the macaques.

To determine the shared and distinct intestinal viruses among the three groups, the gut viral composition at different levels was then compared. At the species level, the Venn diagram showed that 647 of 1048 viral species were shared among the three age groups, while 73, 71, and 40 were exclusive to young, adult, and old cohorts, respectively (Figure 2a). At the family level, the gut DNA virome from the macaques mainly comprised seven families, which was dominated by *Podoviridae*, *Siphoviridae*, *Myoviridae*, and *unclassified_d_virus* families (Figure 2b). Among them, *Podoviridae*, *Siphoviridae*, and *Myoviridae* were assigned to the *Caudovirales* order, the main phage members. To further quantify age-related changes in the gut virome, we compared the relative abundance of the aforementioned phages among the three age groups. Consequently, only one family, *Myoviridae*, was statistically enriched in the young age-group relative to the adult group (one-way ANOVA, p = 0.027), but no significant difference was observed between the young or adult group and the old age-group. The remaining families were not found to differ statistically among the three age groups (one-way ANOVA, all p values >0.05; Figure 2c; Figure A1).
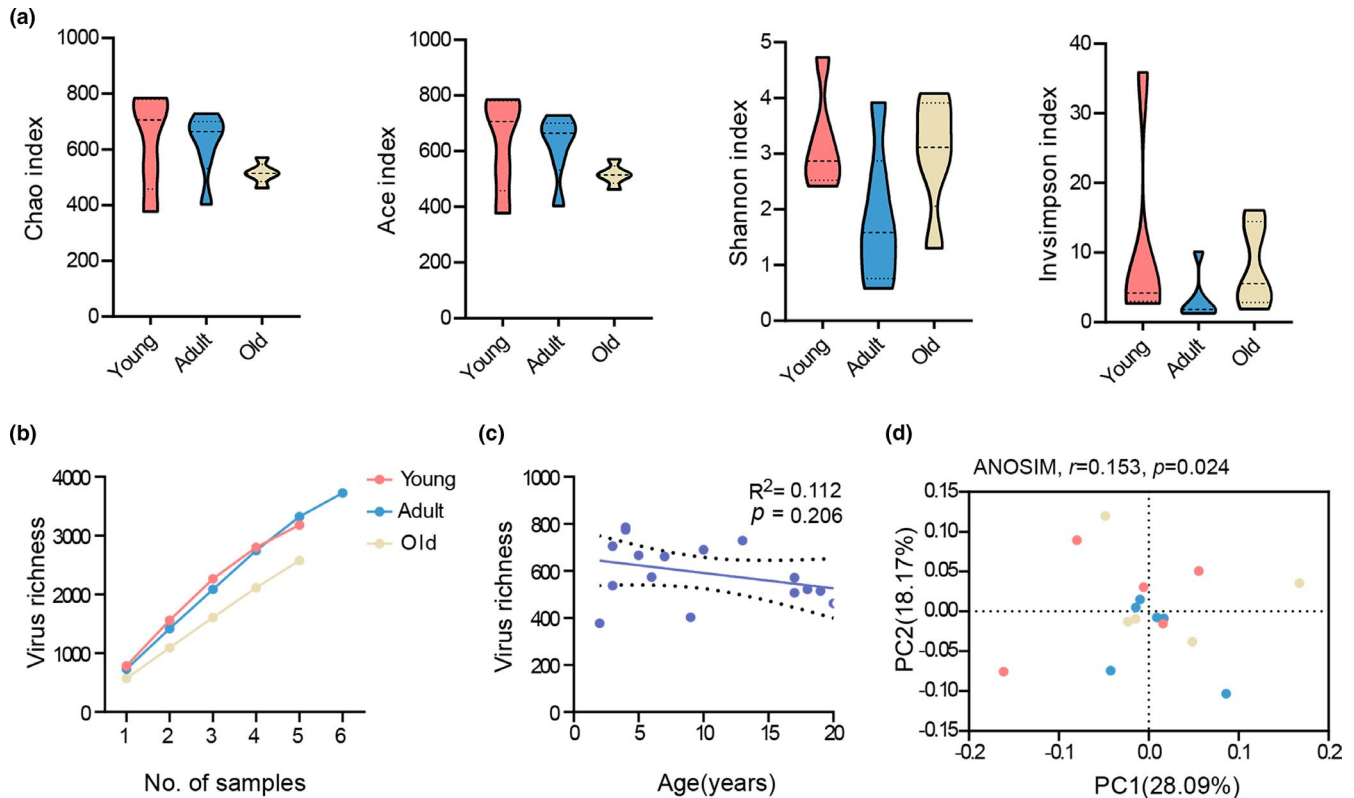
FIGURE 1 The DNA virome biodiversity within the gut metagenome of cynomolgus macaques in the different age-groups. (a) α-diversity analysis showing the lack of statistically significant differences in viral richness (Chao and Ace index) and diversity (Invsimpson and Shannon index) among the three age groups. (b) Rarefaction curves showing the acquisition of viral species richness. (c) Viral species richness at the indicated ages. Linear regression, R^2 value, and 95% confidence intervals were shown. (d) Principal coordinate analysis (PCoA) based on the Abund–Jaccard distances showed a clear separation among the three age groups at the species level (ANOSIM, r = 0.153, p = 0.024). Young, n = 5; adult, n = 6; and old, n = 5

3.4 | Bacteriophage dominance and age-related alterations in the gut DNA virome

The LEfSe analysis was conducted to confirm the profiles of the gut DNA virome in the different age-groups. Altogether, we identified 45 differentially represented viral species responsible for this discrimination (Figure 3a; Table A1). These different species were similarly dominated by phages, most of which were assigned to the _Caudovirales_ order, which included _Myoviridae_ (19 species, 42.22%), _Siphoviridae_ (14 species, 31.11%), and _Podoviridae_ (6 species, 13.33%) families (Figure 3b). Furthermore, the relative abundance of the families (_Myoviridae_ r = −0.662, p = 0.005; _Siphoviridae_ r = −0.562, p = 0.024; and _Podoviridae_ r = −0.535, p = 0.033) decreased significantly with age (Figure 3c).

3.5 | Functional profiles of the age-related gut DNA virome based on KEGG pathway analysis

To outline the functional profiles of the gut DNA virome, we annotated the nonredundant gene set from the gut virome using the KEGG database. In the first-level KEGG pathways, the intestinal viral functions were mainly enriched in genetic information processing

and metabolism (Figure 4a). To further explore the functional profiles of the age-related gut viruses, we performed a PCoA on the third-level KEGG pathways using the Abund–Jaccard distance metric. The ANOSIM results indicated that the KEGG pathways were separated among the three age groups (r = 0.369, p = 0.001; Figure 4b). Using LEfSe analysis, we identified five differential pathways that were mainly involved in pyrimidine metabolism, DNA replication, and folate metabolism among the three age groups (LDA >2.0; Figure 4c; Table A2). Importantly, the broader conclusions were not driven by outliers, which was supported even following the removal of outliers.

3.6 | The relationship between age-related bacteriophages and bacteria

We sought to determine whether the changes we detected in the bacteriophage sequences from the monkey feces at different ages were related to disturbances in the gut microbes. Interestingly, bacteriophage richness was positively correlated with bacterial richness (Spearman's correlation, r = 0.779, p < 0.001; Figure A2a). In contrast, previous research has shown that phage richness is negatively correlated with bacterial diversity in infant monozygotic twins (Moreno-Gallego et al., 2019). Likewise, we found that bacteriophage and
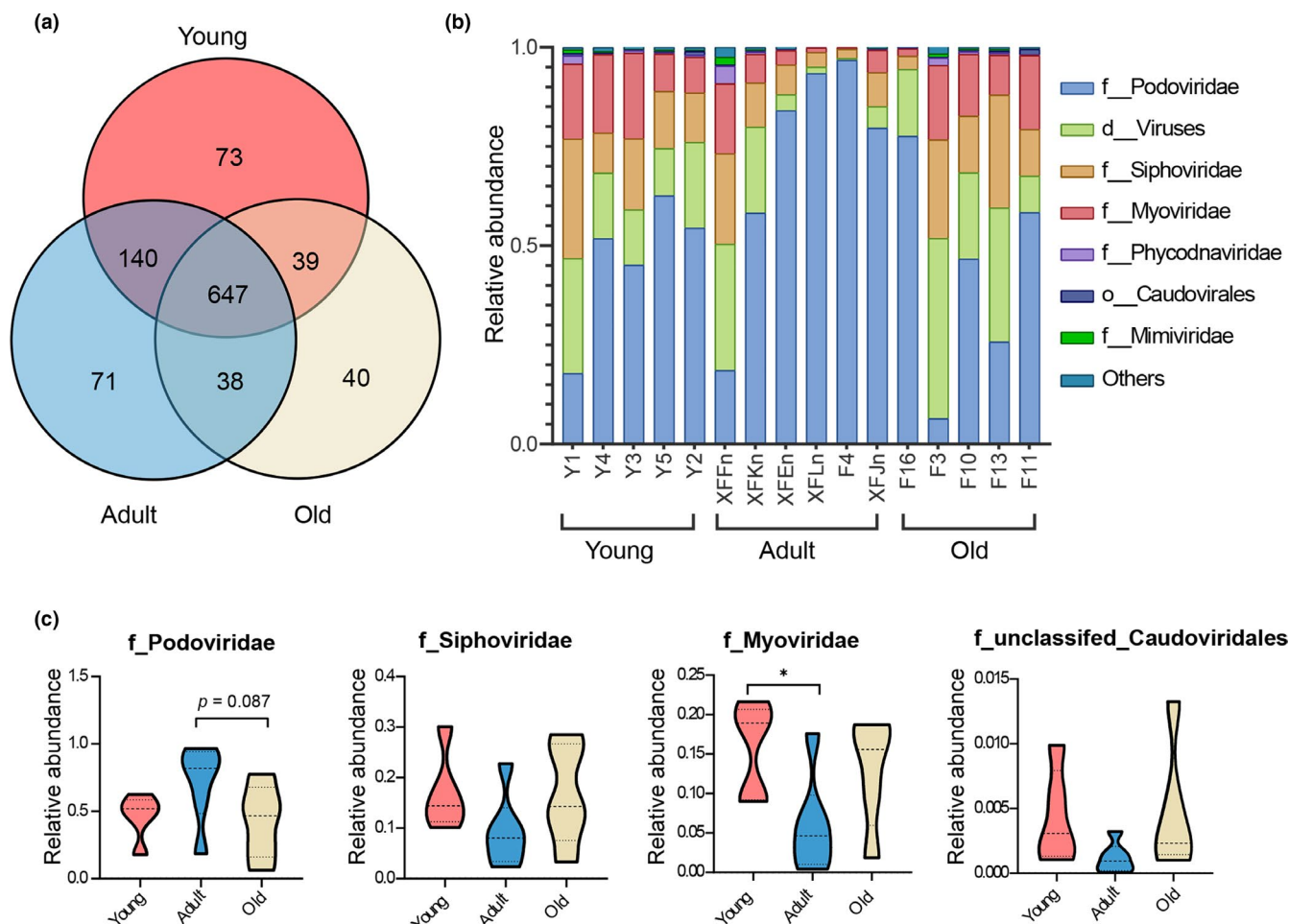
FIGURE 2 The DNA virome at different levels in the gut microbiome of young, adult, and old female cynomolgus. (a) Venn diagram depicting the viral richness and the overlap in viral communities among young (red), adult (blue), and old (yellow) monkeys at the species level. (b) The community bar plot illustrated that the gut DNA virome from cynomolgus macaques mainly contained seven families. (c) Quantification of the relative abundance of the four families assigned to the *Caudovirales* order. Only the *Myoviridae* family was significantly enriched in the young age-group versus the adult group ($p = 0.027$), not the old group. p values were determined by one-way ANOVA followed by LSD's multiple comparison tests. The following n values represented the number of independent animals used for statistical evaluation: young, $n = 5$; adult, $n = 6$; and old, $n = 5$

bacterial diversity were positively related in an age-dependent manner, although no statistical difference was found (Spearman's correlation, $r = 0.147$, $p = 0.587$; Figure A2b). Thus, the intestinal viruses and microbes from cynomolgus monkeys synchronously changed with age.

To further investigate possible correlations between age-related gut phages and bacteria in the healthy monkeys, a co-occurrence network analysis was conducted. We observed that age-related bacteriophages were broadly related to symbiotic bacteria (Figure 5a), with 64.10% (25/39 viral species) of the altered phages showing strong correlations with multiple gut bacteria (related to more than one bacterium $r > \pm 0.7$, $p < 0.001$). Likewise, these phages were mainly assigned to *Myoviridae*, *Siphoviridae*, and *Podoviridae* families. The age-related intestinal bacteriophage members also showed clear correlations with multiple symbiotic bacteria, which were mainly assigned as highly prevalent gut bacteria phyla, including *Firmicutes*, *Proteobacteria*, *Bacteroidetes*, and *Actinobacteria* phyla (Figure 5b;

Table A3). We next identified the hosts of these phages in the NCBI database and, interestingly, most of the hosts were *Firmicutes* or *Proteobacteria* members, but these bacterial hosts and the age-related gut bacteria were inconsistent at the species level (Table A4).

4 | DISCUSSION

We have previously reported that the gut bacteriome in cynomolgus macaques changes with age (Duan et al., 2019). Recently, some studies have reported that a variety of gut viruses, especially tailed bacteriophages, are present in the intestines of healthy mammals (Lawrence et al., 2019). Furthermore, the gut virome is believed to affect mammalian health, but whether dynamic changes occur in them during aging remains unknown. Here, we compared the structure and function of the gut DNA virome in 16 female monkeys at three representative life stages (young, adult, and old), and

(a)

(b)

(c)
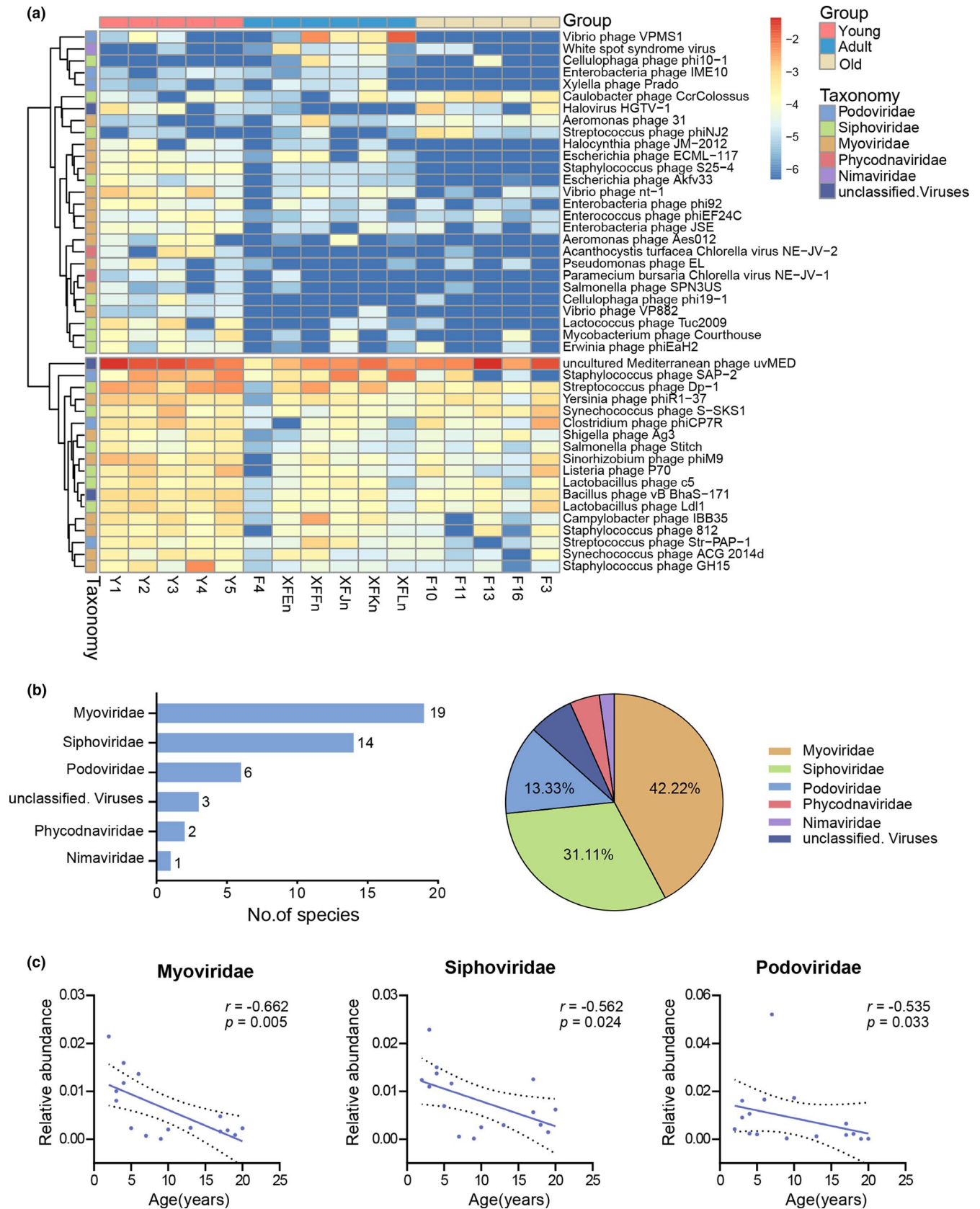
FIGURE 3 The differentially represented viral species among the three groups. (a) Heatmap of the 45 discriminative species' abundances among the young, adult, and old age-groups (LDA > 2.0). Species (raw) were sorted at the family level, and samples (column) were sorted by age. Color intensity (blue to yellow) indicated the score-normalized abundance for each species. (b) The absolute and relative proportion of discriminative species in different families. The intestinal viral species from the monkeys were dominated by phages, the overwhelming majority of which were from the *Caudovirales* order, which comprised *Myoviridae* (42.22%), *Siphoviridae* (31.11%), and *Podoviridae* (13.33%) families. (c) Scatter diagrams showing the relative abundances of the age-related *Myoviridae*, *Siphoviridae*, and *Podoviridae* families, as determined by Spearman's correlation analysis
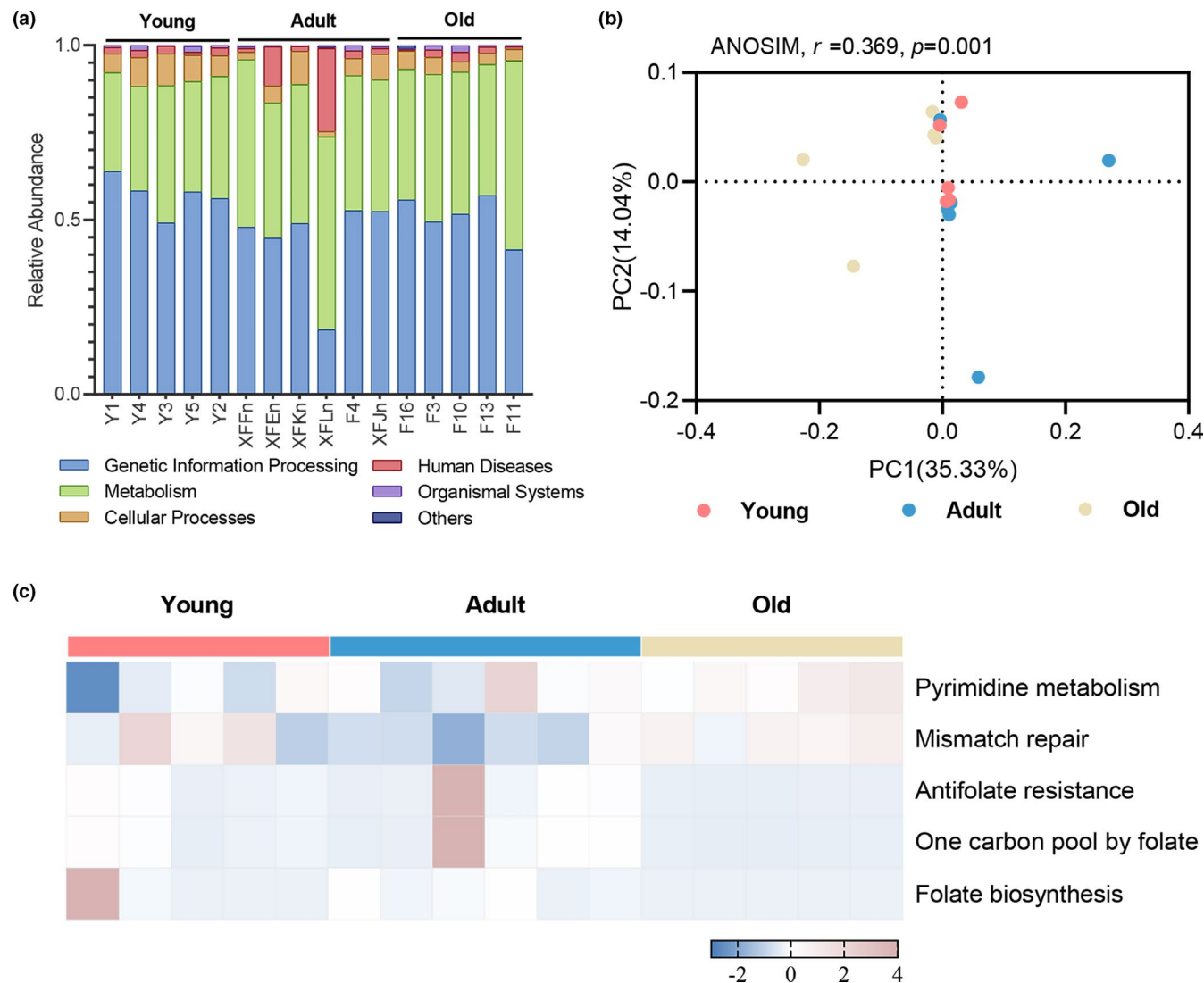
FIGURE 4 The functional profiles of age-related gut DNA virome in the KEGG pathway. (a) Relative abundances of the first-level KEGG pathways in the gut DNA virome. (b) PCoA based on the Abund–Jaccard distance showed clear discrimination among the three groups in the third-level KEGG pathways. (c) Heatmap of the relative abundances of the five differential pathways among the young, adult, and old age-groups (LDA > 2.0). Functional profiles in the DNA virome were enriched in pyrimidine metabolism, DNA replication, and folate metabolism

found that the gut DNA virome dramatically changed with age. The most abundant gut viruses, which were bacteriophages within the *Caudovirales* order, included *Siphoviridae*, *Myoviridae*, and *Podoviridae* families, a finding consistent with previous reports (Norman et al., 2015; Shkoporov & Hill, 2019). Moreover, there was a broad and strong interaction between the age-related gut bacteriophages and bacteria, the latter of which were highly prevalent gut microbes such as *Firmicutes*, *Bacteroidetes*, *Proteobacteria*, and *Actinobacteria* phyla. Overall, our findings augment the current understanding of the effect of aging on the structure and function of the gut virome in non-human primates.

The gut virome in humans is personalized and stable and it is dominated by phages (Shkoporov et al., 2019). Previous studies have reported that bacteriophages from the human intestinal mucosa or stools mainly contain double-stranded (ds) DNA and single-stranded (ss) DNA phages. dsDNA phages generally comprise *Siphoviridae*,

Podoviridae, and *Myoviridae* families, whereas ssDNA phages are mostly *Microviridae* family members (Shkoporov & Hill, 2019). Here, we found that the gut DNA virome in healthy female monkeys was dominated by *Siphoviridae*, *Myoviridae*, and *Podoviridae* families, which was partly consistent with previous studies, underscoring the notion that virus–host interactions cannot be solely considered as pathogenic. Nonetheless, the fact that we were unable to identify ssDNA bacteriophages in the gut DNA virome was probably accounted for low viral loads and inadequate nucleic acid extraction procedures. For instance, it is known that the ssDNA genome is unstable and easily degraded (Minot et al., 2013), and *Microviridae* virions form circular DNA packaged in icosahedral capsids.

To date, two major bacteriome–phageome dynamics have been detected by researchers that elucidate some aspects of the dynamic changes that occur in the phage community and phage–bacteria co-evolution. Among them, one is the "piggyback-the-winner" model
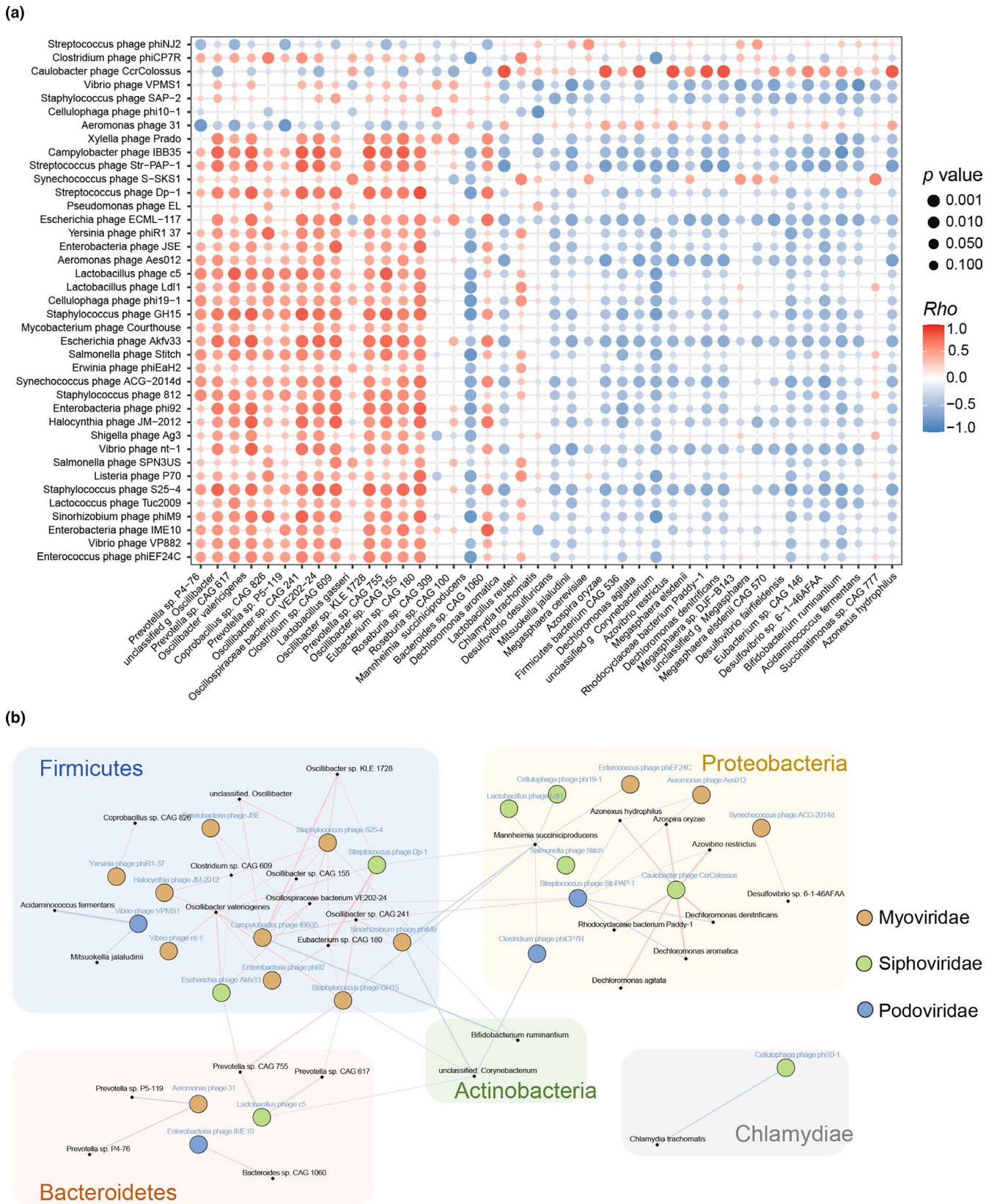
FIGURE 5 Correlations between gut bacteriophages and bacteria. (a) Association between 39 different bacteriophages and 42 discriminative bacteria identified by LEfSe analysis of the metagenomic sequences (LDA > 2.0). The size and color of each scatter plot point showed the *p* values of Spearman's correlation (ranging from 9.87e–06 to 0.99) and correlation coefficient values (ranging from −0.867 to 0.874) between the different bacteriophages and bacteria, respectively. (b) Co-occurrence network deduced from the relationship between the age-related bacteriophages and bacteria. Circles and dots represented the different bacteriophages and bacteria, respectively. Circle colors varied according to the viral family. Bacterial species that were annotated at the phylum level were marked. Lines between nodes indicated Spearman's negative (light blue) or positive (light red) correlation, and line thickness indicated the *p*-value (*p* < 0.001)

(Shkoporov & Hill, 2019; Silveira & Rohwer, 2016), whereby intestinal phages are dominated by lysogenic phages, resulting in a stable virus to microbe ratio; the other is the "kill-the-winner" model (Beller & Matthijnssens, 2019; Rodriguez-Valera et al., 2009), in which virulent phages replicate and proliferate within host bacteria, leading to decreased bacterial loads by lysing their hosts. Our results showed that bacteriophage richness was positively correlated with bacterial richness, which was consistent with the former model, suggesting that most intestinal bacteriophages in our study might retain lysogenic or lysogeny-like interactions with their hosts (Mills et al., 2013). Despite their high metabolic consumption requirements, lysogenic phages can beneficially alter the physiological characteristics of host bacteria (Brussow et al., 2004). Therefore, intestinal phages do more than just act as predators; in some cases, they help to maintain gut microbial homeostasis by integrating genes that carry competitive advantages into the symbiotic genome of the host (Mills et al., 2013; Modi et al., 2013).

Herein, age-related bacteriophages formed a broad and strong co-occurring relationship with highly prevalent gut microbes from the *Firmicutes*, *Bacteroidetes*, *Proteobacteria*, and *Actinobacteria* phyla. Consistent with this, previous studies have found that members of the *Siphoviridae* family are capable of infecting some intestinal microbes such as *Bacteroides* and *Clostridium* in humans (Gilbert et al., 2017; Gómez-Doñate et al., 2011; Ramírez-Vargas et al., 2018). A recent study also reported that *Myoviridae* viral particle types can be induced and identified from human intestinal *Bifidobacterium* (Mavrich et al., 2018). This inferred that the abundance of phages in a given environment may reflect the abundance of their symbiotic host bacteria (Breitbart & Rohwer, 2005).

Unlike the gut bacteriome, which was enriched in genes associated with arginine biosynthesis, purine metabolism, microbial polysaccharide metabolism, and gut viral functions were enriched for genetic information processing and nucleotide and folate metabolism. Intestinal bacteriophages are capable of modulating the functions of prokaryotic communities by the integration into prokaryotic genomes. For example, gene integration can directly affect bacterial hosts, resulting in cascading effects on other intestinal bacterial species, with consequential alteration of the gut microbiome (Hsu et al., 2019). Thus, further efforts will be required to clarify the complex interacting effect of the gut virome on the gut bacteriomes.

Interestingly, we found that the richness of gut DNA virome in female cynomolgus generally tended to decline with age, especially the *Caudovirales* order, resulting in lower bacterial biodiversity in old monkeys. Generally speaking, high biodiversity is equal to good health status (Huttenhower et al., 2012). The downregulated *Caudovirales* order was related to the altered intestinal folate metabolism. A multicenter study has shown that functional folate deficiency increases with age in inpatients (Mézière et al., 2014). Our findings suggest that modulating the intestinal virome may be beneficial for the treatment of aging.

There were some limitations in our study. First, we did not sequence the RNA virome, which is increasingly recognized as an important component of the gut microbiome that is involved in health and disease (Virgin, 2014). Therefore, future studies should investigate changes in the gut RNA virome with age. Second, due to the low reproductive rate and morbidity, as well as ethical considerations, the sample sizes were relatively small; thus, the reliability of the association reported may be impacted. Finally, the dynamic changes we observed in the gut virome with age require in-depth validation.

5 | CONCLUSIONS

In summary, we profiled structural and functional alterations of the gut DNA virome associated with age in non-human primates. We found that the gut DNA virome differed significantly among the three age groups, as observed in alterations in the viral functional pathways related to nucleotide and folate metabolism. The gut virome was dominated by dsDNA phages, especially the *Caudovirales* order, which showed strong correlations with the highly prevalent gut bacteria. Herein, age-related gut bacteriophages and bacteria were in a complementary relationship, and both of them decreased in richness during aging. We thus speculated that certain bacteriophage supplementation may be beneficial for the treatment of aging through modulating the structure and function of the intestinal flora in mammals.

AUTHOR CONTRIBUTIONS

Xunmin Tan: Formal analysis (equal); Visualization (equal); Writing-original draft (equal). **Tingjia Chai:** Formal analysis (equal); Visualization (equal); Writing-original draft (equal). **Jiajia Duan:** Writing-review & editing (equal). **Jing Wu:** Data curation (equal); Software (equal). **Hanping Zhang:** Data curation (equal); Software (equal). **Yifan Li:** Data curation (equal); Software (equal). **Yu Huang:** Data curation (equal); Software (equal). **Xi Hu:** Data curation (equal); Software (equal). **Peng Zheng:** Writing-review & editing (equal).

Jinlin Song: Validation (equal). **Ping Ji:** Validation (equal). **Xin Jin:** Validation (equal). **Hongmei Zhang:** Validation (equal). **Peng Xie:** Conceptualization (lead); Funding acquisition (lead); Supervision (lead); Writing-review & editing (equal).

DATA AVAILABILITY STATEMENT

ORCID

Peng Xie https://orcid.org/0000-0002-0081-6048

REFERENCES

Appt, S. E., Chen, H., Goode, A. K., Hoyer, P. B., Clarkson, T. B., Adams, M. R., Wilson, M. E., Franke, A. A., & Kaplan, J. R. (2010). The effect of diet and cardiovascular risk on ovarian aging in cynomolgus monkeys (_Macaca fascicularis_). _Menopause_, _17_, 741–748.

Barton, E. S., White, D. W., Cathelyn, J. S., Brett-Mcclellan, K. A., Engle, M., Diamond, M. S., Miller, V. L., & Virgin, H. W. T. (2007). Herpesvirus latency confers symbiotic protection from bacterial infection. _Nature_, _447_, 326–329.

Beller, L., & Matthijnssens, J. (2019). What is (not) known about the dynamics of the human gut virome in health and disease. _Current Opinion in Virology_, _37_, 52–57.

Biagi, E., Nylund, L., Candela, M., Ostan, R., Bucci, L., Pini, E., Nikkila, J., Monti, D., Satokari, R., Franceschi, C., Brigidi, P., & de Vos, W. (2010). Through ageing, and beyond: gut microbiota and inflammatory status in seniors and centenarians. _PLoS One_, _5_, e10667.

Breitbart, M., & Rohwer, F. (2005). Here a virus, there a virus, everywhere the same virus? _Trends in Microbiology_, _13_, 278–284.

Brussow, H., Canchaya, C., & Hardt, W. D. (2004). Phages and the evolution of bacterial pathogens: From genomic rearrangements to lysogenic conversion. _Microbiology and Molecular Biology Reviews_, _68_(3), 560–602.

Drevon-Gaillot, E., Perron-Lepage, M. F., Clement, C., & Burnett, R. (2006). A review of background findings in cynomolgus monkeys (_Macaca fascicularis_) from three different geographical origins. _Experimental and Toxicologic Pathology_, _58_, 77–88.

Duan, J., Yin, B., Li, W., Chai, T., Liang, W., Huang, Y., Tan, X., Zheng, P., Wu, J., Li, Y., Li, Y., Zhou, W., & Xie, P. (2019). Age-related changes in microbial composition and function in cynomolgus macaques. _Aging_, _11_, 12080–12096.

Flemer, B., Lynch, D. B., Brown, J. M., Jeffery, I. B., Ryan, F. J., Claesson, M. J., O'Riordain, M., Shanahan, F., & O'Toole, P. W. (2017). Tumour-associated and non-tumour-associated microbiota in colorectal cancer. _Gut_, _66_, 633–643.

Gentile, C. L., & Weir, T. L. (2018). The gut microbiota at the intersection of diet and human health. _Science_, _362_, 776–780.

Gilbert, R. A., Kelly, W. J., Altermann, E., Leahy, S. C., Minchin, C., Ouwerkerk, D., & Klieve, A. V. (2017). Toward understanding phage: Host interactions in the rumen; complete genome sequences of lytic phages infecting rumen bacteria. _Frontiers in Microbiology_, _8_, 2340.

Gómez-Doñate, M., Payán, A., Cortés, I., Blanch, A. R., Lucena, F., Jofre, J., & Muniesa, M. (2011). Isolation of bacteriophage host strains of Bacteroides species suitable for tracking sources of animal fecal pollution in water. _Environmental Microbiology_, _13_, 1622–1631.

Górska, A., Peter, S., Willmann, M., Autenrieth, I., Schlaberg, R., & Huson, D. H. (2018). Dynamics of the human gut phageome during antibiotic treatment. _Computational Biology and Chemistry_, _74_, 420–427.

Hsu, B. B., Gibson, T. E., Yeliseyev, V., Liu, Q., Lyon, L., Bry, L., Silver, P. A., & Gerber, G. K. (2019). Dynamic modulation of the gut microbiota and metabolome by bacteriophages in a mouse model. _Cell Host & Microbe_, _25_, 803–814.e5.

Huttenhower, C., Gevers, D., Knight, R., Abubucker, S., Badger, J. H., & Chinwalla, A. T. (2012). Structure, function and diversity of the healthy human microbiome. _Nature_, _486_, 207–214.

Lawrence, D., Baldridge, M. T., & Handley, S. A. (2019). Phages and Human Health: More Than Idle Hitchhikers. _Viruses_, _11_(7), 587. https://doi.org/10.3390/v11070587

Li, R., Li, Y., Kristiansen, K., & Wang, J. (2008). SOAP: Short oligonucleotide alignment program. _Bioinformatics_, _24_, 713–714.

Lim, E. S., Zhou, Y., Zhao, G., Bauer, I. K., Droit, L., Ndao, I. M., Warner, B. B., Tarr, P. I., Wang, D., & Holtz, L. R. (2015). Early life dynamics of the human gut virome and bacterial microbiome in infants. _Nature Medicine_, _21_, 1228–1234.

Lynch, S. V., & Pedersen, O. (2016). The human intestinal microbiome in health and disease. _New England Journal of Medicine_, _375_, 2369–2379.

Matson, V., Fessler, J., Bao, R., Chongsuwat, T., Zha, Y., Alegre, M. L., Luke, J. J., & Gajewski, T. F. (2018). The commensal microbiome is associated with anti-PD-1 efficacy in metastatic melanoma patients. _Science_, _359_, 104–108.

Mavrich, T. N., Casey, E., Oliveira, J., Bottacini, F., James, K., Franz, C., Lugli, G. A., Neve, H., Ventura, M., Hatfull, G. F., Mahony, J., & van Sinderen, D. (2018). Characterization and induction of prophages in human gut-associated Bifidobacterium hosts. _Scientific Reports_, _8_, 12772.

Mézière, A., Audureau, E., Vairelles, S., Krypciak, S., Dicko, M., Monié, M., & Giraudier, S. (2014). B12 deficiency increases with age in hospitalized patients: a study on 14,904 samples. _Journals of Gerontology. Series A_, _Biological Sciences and Medical Sciences_, _69_, 1576–1585.

Mills, S., Shanahan, F., Stanton, C., Hill, C., Coffey, A., & Ross, R. P. (2013). Movers and shakers: Influence of bacteriophages in shaping the mammalian gut microbiota. _Gut Microbes_, _4_, 4–16.

Minot, S., Bryson, A., Chehoud, C., Wu, G. D., Lewis, J. D., & Bushman, F. D. (2013). Rapid evolution of the human gut virome. _Proceedings of the National Academy of Sciences of the United States of America_, _110_, 12450–12455.

Minot, S., Sinha, R., Chen, J., Li, H., Keilbaugh, S. A., Wu, G. D., Lewis, J. D., & Bushman, F. D. (2011). The human gut virome: Inter-individual variation and dynamic response to diet. _Genome Research_, _21_, 1616–1625.

Modi, S. R., Lee, H. H., Spina, C. S., & Collins, J. J. (2013). Antibiotic treatment expands the resistance reservoir and ecological network of the phage metagenome. _Nature_, _499_, 219–222.

Moreno-Gallego, J. L., Chou, S. P., di Rienzi, S. C., Goodrich, J. K., Spector, T. D., Bell, J. T., Youngblut, N. D., Hewson, I., Reyes, A., & Ley, R. E. (2019). Virome diversity correlates with intestinal microbiome diversity in adult monozygotic twins. _Cell Host & Microbe_, _25_, 261–272.e5.

Norman, J. M., Handley, S. A., Baldridge, M. T., Droit, L., Liu, C. Y., Keller, B. C., Kambal, A., Monaco, C. L., Zhao, G., Fleshner, P., Stappenbeck, T. S., McGovern, D. P., Keshavarzian, A., Mutlu, E. A., Sauk, J., Gevers, D., Xavier, R. J., Wang, D., Parkes, M., & Virgin, H. W. (2015). Disease-specific alterations in the enteric virome in inflammatory bowel disease. _Cell_, _160_, 447–460.

Qiu, C., Kivipelto, M., & von Strauss, E. (2009). Epidemiology of Alzheimer's disease: Occurrence, determinants, and strategies toward intervention. _Dialogues in Clinical Neuroscience_, _11_, 111–128.

Ramírez-Vargas, G., Goh, S., & Rodríguez, C. (2018). The novel phages phiCD5763 and phiCD2955 represent two groups of big plasmidial siphoviridae phages of _Clostridium difficile_. _Frontiers in Microbiology_, _9_, 26.

Rampelli, S., Turroni, S., Schnorr, S. L., Soverini, M., Quercia, S., Barone, M., Castagnetti, A., Biagi, E., Gallinella, G., Brigidi, P., & Candela, M. (2017). Characterization of the human DNA gut virome across populations with different subsistence strategies and geographical origin. *Environmental Microbiology*, 19, 4728–4735.

Rodriguez-Valera, F., Martin-Cuadrado, A. B., Rodriguez-Brito, B., Pasić, L., Thingstad, T. F., Rohwer, F., & Mira, A. (2009). Explaining microbial population genomics through phage predation. *Nature Reviews Microbiology*, 7, 828–836.

Sampson, T. R., Debelius, J. W., Thron, T., Janssen, S., Shastri, G. G., Ilhan, Z. E., Challis, C., Schretter, C. E., Rocha, S., Gradinaru, V., Chesselet, M. F., Keshavarzian, A., Shannon, K. M., Krajmalnik-Brown, R., Wittung-Stafshede, P., Knight, R., & Mazmanian, S. K. (2016). Gut microbiota regulate motor deficits and neuroinflammation in a model of Parkinson's disease. *Cell*, 167, 1469–1480.e12.

Segata, N., Izard, J., Waldron, L., Gevers, D., Miropolsky, L., Garrett, W. S., & Huttenhower, C. (2011). Metagenomic biomarker discovery and explanation. *Genome Biology*, 12, R60.

Sharma, V., Smolin, J., Nayak, J., Ayala, J. E., Scott, D. A., Peterson, S. N., & Freeze, H. H. (2018). Mannose alters gut microbiome, prevents diet-induced obesity, and improves host metabolism. *Cell Reports*, 24, 3087–3098.

Sharon, G., Cruz, N. J., Kang, D. W., Gandal, M. J., Wang, B., Kim, Y. M., Zink, E. M., Casey, C. P., Taylor, B. C., Lane, C. J., Bramer, L. M., Isern, N. G., Hoyt, D. W., Noecker, C., Sweredoski, M. J., Moradian, A., Borenstein, E., Jansson, J. K., Knight, R., ... Mazmanian, S. K. (2019). Human gut microbiota from autism spectrum disorder promote behavioral symptoms in mice. *Cell*, 177(1600–1618), e17.

Shaw, A. C., Goldstein, D. R., & Montgomery, R. R. (2013). Age-dependent dysregulation of innate immunity. *Nature Reviews Immunology*, 13, 875–887.

Shkoporov, A. N., Clooney, A. G., Sutton, T. D. S., Ryan, F. J., Daly, K. M., Nolan, J. A., McDonnell, S. A., Khokhlova, E. V., Draper, L. A., Forde, A., Guerin, E., Velayudhan, V., Ross, R. P., & Hill, C. (2019). The human gut virome is highly diverse, stable, and individual specific. *Cell Host & Microbe*, 26, 527–541.e5.

Shkoporov, A. N., & Hill, C. (2019). Bacteriophages of the human gut: The "known unknown" of the microbiome. *Cell Host & Microbe*, 25, 195–209.

Silveira, C. B., & Rohwer, F. L. (2016). Piggyback-the-Winner in host-associated microbial communities. *NPJ Biofilms Microbiomes*, 2, 16010.

Virgin, H. W. (2014). The virome in mammalian physiology and disease. *Cell*, 157, 142–150.

Wang, J. C., & Bennett, M. (2012). Aging and atherosclerosis: mechanisms, functional consequences, and potential therapeutics for cellular senescence. *Circulation Research*, 111, 245–259.

Wang, S., Zheng, Y., Li, J., Yu, Y., Zhang, W., Song, M., Liu, Z., Min, Z., Hu, H., Jing, Y., He, X., Sun, L., Ma, L., Esteban, C. R., Chan, P., Qiao, J., Zhou, Q., Izpisua Belmonte, J. C., Qu, J., Tang, F., & Liu, G. H. (2020). Single-cell transcriptomic atlas of primate ovarian aging. *Cell*, 180(585–600), e19.

Xie, C., Mao, X., Huang, J., Ding, Y., Wu, J., Dong, S., Kong, L., Gao, G., Li, C. Y., & Wei, L. (2011). KOBAS 2.0: A web server for annotation and identification of enriched pathways and diseases. *Nucleic Acids Research*, 39, W316–W322.

Xu, F., Xie, L., Li, X., Li, Q., Wang, T., Ji, Y., Kong, F., Zhan, Q., Cheng, K., Fang, L., & Xie, P. (2012). Construction and validation of a systematic ethogram of *Macaca fascicularis* in a free enclosure. *PLoS One*, 7, e37486.

Yang, J., Zheng, P., Li, Y., Wu, J., Tan, X., Zhou, J., Sun, Z., Chen, X., Zhang, G., Zhang, H., Huang, Y., Chai, T., Duan, J., Liang, W., Yin, B., Lai, J., Huang, T., Du, Y., Zhang, P., ... Xie, P. (2020). Landscapes of bacterial and metabolic signatures and their interaction in major depressive disorders. *Science Advances*, 6.

Zheng, P., Wu, J., Zhang, H., Perry, S. W., Yin, B., Tan, X., Chai, T., Liang, W., Huang, Y., Li, Y., Duan, J., Wong, M. L., Licinio, J., & Xie, P. (2020). The gut microbiome modulates gut-brain axis glycerophospholipid metabolism in a region-specific manner in a nonhuman primate model of depression. *Molecular Psychiatry*. https://doi.org/10.1038/s41380-020-0744-2

APPENDIX 1

TABLE A1　The discriminative species of the gut DNA virome among the young, adult, and old groups

| Species | Family | Relative abundance | | | | | | p-value | LDA | Enrichment |
		Young (mean)	Young (SD)	Adult (mean)	Adult (SD)	Old (mean)	Old (SD)			
Enterococcus phage phiEF24C	*Myoviridae*	1.8E-04	1.7E-04	2.0E-05	1.8E-05	3.9E-05	4.7E-05	0.015	2.124	Young
Vibrio phage VP882	*Myoviridae*	3.3E-05	2.1E-05	9.3E-06	2.1E-05	0.0E+00	0.0E+00	0.008	2.383	Young
Enterobacteria phage IME10	*Podoviridae*	2.2E-05	1.8E-05	1.6E-05	1.1E-05	0.0E+00	0.0E+00	0.029	2.888	Young
Sinorhizobium phage phiM9	*Myoviridae*	2.2E-03	1.4E-03	2.1E-04	2.4E-04	5.0E-04	6.8E-04	0.028	2.964	Young
Lactococcus phage Tuc2009	*Siphoviridae*	8.3E-04	8.2E-04	1.4E-05	1.9E-05	4.1E-06	8.2E-06	0.041	2.594	Young

| Species | Family | Relative abundance | | | | | | p-value | LDA | Enrichment |
		Young (mean)	Young (SD)	Adult (mean)	Adult (SD)	Old (mean)	Old (SD)			
Staphylococcus phage S25-4	_Myoviridae_	3.3E-04	5.8E-05	2.1E-05	1.2E-05	0.0E+00	0.0E+00	0.002	2.806	Young
Listeria phage P70	_Siphoviridae_	1.9E-03	1.5E-03	1.4E-04	1.2E-04	9.7E-04	1.4E-03	0.046	2.949	Young
Salmonella phage SPN3US	_Myoviridae_	2.2E-05	2.3E-05	1.7E-06	3.7E-06	1.6E-06	3.1E-06	0.047	2.644	Young
Paramecium bursaria Chlorella virus NE-JV-1	_Phycodnaviridae_	4.5E-05	4.5E-05	6.7E-06	1.5E-05	0.0E+00	0.0E+00	0.023	2.563	Young
Vibrio phage nt-1	_Myoviridae_	1.4E-03	1.3E-03	1.1E-04	1.1E-04	2.0E-05	2.6E-05	0.016	2.866	Young
Shigella phage Ag3	_Myoviridae_	5.4E-04	3.2E-04	8.3E-05	8.8E-05	1.8E-04	1.8E-04	0.034	2.505	Young
Halocynthia phage JM-2012	_Myoviridae_	1.2E-04	1.0E-04	1.1E-05	1.2E-05	0.0E+00	0.0E+00	0.020	2.097	Young
Enterobacteria phage phi92	_Myoviridae_	2.1E-04	1.2E-04	4.6E-05	5.2E-05	1.5E-05	1.5E-05	0.016	2.312	Young
Acanthocystis turfacea Chlorella virus NE-JV-2	_Phycodnaviridae_	4.4E-04	5.5E-04	0.0E+00	0.0E+00	1.6E-06	3.1E-06	0.011	2.387	Young
Staphylococcus phage 812	_Myoviridae_	6.6E-04	2.9E-04	1.4E-04	8.1E-05	2.9E-04	3.5E-04	0.037	2.454	Young
Synechococcus phage ACG 2014d	_Myoviridae_	6.4E-04	3.4E-04	2.2E-04	2.5E-04	1.1E-04	1.4E-04	0.031	2.483	Young
Erwinia phage phiEaH2	_Siphoviridae_	1.4E-04	1.0E-04	1.1E-05	2.0E-05	4.8E-05	8.0E-05	0.035	2.345	Young
Salmonella phage Stitch	_Siphoviridae_	4.6E-04	2.9E-04	7.8E-05	7.7E-05	1.3E-04	1.1E-04	0.032	2.336	Young
Escherichia phage Akfv33	_Siphoviridae_	1.4E-04	1.4E-04	1.6E-05	8.9E-06	3.6E-07	7.2E-07	0.004	2.529	Young
Mycobacterium phage Courthouse	_Siphoviridae_	4.1E-04	4.8E-04	3.8E-05	6.4E-05	3.8E-05	7.6E-05	0.026	2.459	Young
Staphylococcus phage GH15	_Myoviridae_	2.8E-03	4.6E-03	6.0E-05	3.5E-05	4.1E-05	2.8E-05	0.010	3.224	Young
Cellulophaga phage phi19-1	_Siphoviridae_	1.2E-04	1.7E-04	0.0E+00	0.0E+00	4.1E-06	8.2E-06	0.001	2.038	Young
Lactobacillus phage Ldl1	_Siphoviridae_	1.5E-03	8.3E-04	2.0E-04	1.3E-04	7.6E-04	9.4E-04	0.022	2.803	Young
Lactobacillus phage c5	_Siphoviridae_	8.0E-04	5.3E-04	2.3E-04	2.0E-04	2.3E-04	1.8E-04	0.020	2.518	Young
Aeromonas phage Aes012	_Myoviridae_	1.9E-04	2.0E-04	3.7E-05	8.1E-05	0.0E+00	0.0E+00	0.031	2.346	Young
Enterobacteria phage JSE	_Myoviridae_	2.1E-04	1.1E-04	3.6E-05	4.3E-05	2.5E-05	3.0E-05	0.013	2.355	Young
uncultured Mediterranean phage uvMED	_unclassified Viruses_	4.2E-02	2.1E-02	1.0E-02	6.7E-03	3.5E-02	3.2E-02	0.029	4.202	Young
Bacillus phage vB BhaS-171	_unclassified Viruses_	1.8E-03	4.7E-04	2.5E-04	1.9E-04	4.7E-04	4.4E-04	0.009	2.906	Young
Yersinia phage phiR1-37	_Myoviridae_	2.2E-03	1.0E-03	5.3E-04	5.0E-04	8.6E-04	6.0E-04	0.041	2.898	Young

TABLE A1 (Continued)

Species	Family	Relative abundance						p-value	LDA	Enrichment
		Young (mean)	Young (SD)	Adult (mean)	Adult (SD)	Old (mean)	Old (SD)			
Escherichia phage ECML-117	*Myoviridae*	1.6E-04	1.1E-04	1.5E-04	1.5E-04	0.0E+00	0.0E+00	0.013	2.210	Young
Pseudomonas phage EL	*Myoviridae*	1.5E-04	2.3E-04	2.3E-06	3.3E-06	9.7E-06	1.2E-05	0.049	2.364	Young
Streptococcus phage Dp-1	*Siphoviridae*	7.3E-03	3.5E-03	2.8E-03	3.3E-03	8.8E-04	4.2E-04	0.033	3.526	Young
Synechococcus phage S-SKS1	*Siphoviridae*	1.3E-03	1.5E-03	2.0E-04	1.3E-04	1.2E-03	1.3E-03	0.025	2.749	Young
Streptococcus phage Str-PAP-1	*Podoviridae*	4.5E-04	2.4E-04	6.0E-04	8.7E-04	5.4E-05	5.3E-05	0.028	2.504	Adult
Campylobacter phage IBB35	*Myoviridae*	1.3E-03	7.5E-04	1.4E-03	2.7E-03	7.9E-05	7.0E-05	0.020	2.865	Adult
Xylella phage Prado	*Podoviridae*	9.4E-06	5.9E-06	5.0E-05	6.8E-05	0.0E+00	0.0E+00	0.042	3.018	Adult
Aeromonas phage 31	*Myoviridae*	8.4E-06	6.9E-06	3.7E-04	7.7E-04	1.1E-04	4.3E-05	0.014	2.558	Adult
Cellulophaga phage phi10-1	*Siphoviridae*	0.0E+00	0.0E+00	2.1E-04	4.1E-04	3.5E-05	7.0E-05	0.029	2.248	Adult
White spot syndrome virus	*Nimaviridae*	3.2E-06	6.4E-06	3.0E-04	4.5E-04	1.6E-05	2.0E-05	0.042	2.430	Adult
Staphylococcus phage SAP-2	*Podoviridae*	6.3E-03	5.0E-03	6.4E-03	8.3E-03	4.4E-04	8.1E-04	0.035	3.472	Adult
Vibrio phage VPMS1	*Podoviridae*	7.4E-05	1.2E-04	7.7E-03	1.2E-02	0.0E+00	0.0E+00	0.023	3.522	Adult
Caulobacter phage CcrColossus	*Siphoviridae*	8.5E-05	7.5E-05	1.3E-04	2.4E-04	9.5E-04	7.9E-04	0.020	2.728	Old
Halovirus HGTV-1	*unclassified Viruses*	3.6E-04	5.5E-04	4.3E-06	7.1E-06	7.2E-04	1.1E-03	0.050	2.381	Old
Clostridium phage phiCP7R	*Podoviridae*	1.6E-03	1.0E-03	1.5E-04	1.5E-04	1.7E-03	2.4E-03	0.042	2.884	Old
Streptococcus phage phiNJ2	*Siphoviridae*	7.5E-06	9.3E-06	1.5E-05	2.6E-05	4.6E-04	6.1E-04	0.034	2.449	Old

TABLE A2 The differential KEGG pathways among the three age groups

KEGG pathway	Relative abundance						p-value	LDA	Enrichment
	Young (mean)	Young (SD)	Adult (mean)	Adult (SD)	Old (mean)	Old (SD)			
Mismatch repair	1.4E-01	3.3E-02	9.9E-02	1.7E-02	1.4E-01	1.1E-02	0.034	4.366	Young
Folate biosynthesis	1.6E-02	3.1E-02	3.3E-03	2.3E-03	0.0E+00	0.0E+00	0.014	4.293	Young
Antifolate resistance	4.5E-03	3.8E-03	1.7E-02	3.0E-02	3.0E-04	2.7E-04	0.018	4.511	Adult
One carbon pool by folate	4.5E-03	3.7E-03	1.8E-02	3.1E-02	3.0E-04	2.7E-04	0.009	4.516	Adult
Pyrimidine metabolism	1.8E-01	4.6E-02	2.2E-01	4.5E-02	2.3E-01	2.1E-02	0.017	4.801	Old

TABLE A3 The discriminative bacterial species among the three groups

Species	Phylum	Relative abundance						p-value	LDA	Enrichment
		Young (mean)	Young (SD)	Adult (mean)	Adult (SD)	Old (mean)	Old (SD)			
Bifidobacterium ruminantium	Actinobacteria	6.59E-06	3.09E-06	2.52E-05	4.15E-05	2.40E-04	4.13E-04	0.024	2.103	Old
unclassified g Corynebacterium	Actinobacteria	5.86E-08	5.07E-08	1.60E-06	3.13E-06	6.25E-04	1.25E-03	0.049	2.451	Old
Bacteroides sp. CAG 1060	Bacteroidetes	5.08E-03	2.12E-03	5.21E-03	2.60E-03	1.12E-03	6.64E-04	0.015	3.317	Adult
Prevotella sp. CAG 617	Bacteroidetes	7.26E-04	2.18E-04	4.69E-04	1.81E-04	3.17E-04	1.65E-04	0.039	2.298	Young
Prevotella sp. CAG 755	Bacteroidetes	1.03E-03	3.96E-04	6.87E-04	3.07E-04	4.71E-04	2.31E-04	0.035	2.439	Young
Prevotella sp. P4-76	Bacteroidetes	1.79E-03	4.11E-04	1.10E-03	4.68E-04	8.80E-04	4.25E-04	0.028	2.647	Young
Prevotella sp. P5-119	Bacteroidetes	1.82E-03	4.25E-04	1.25E-03	4.52E-04	9.92E-04	4.97E-04	0.039	2.602	Young
Chlamydia trachomatis	Chlamydiae	6.01E-03	1.23E-03	3.48E-03	1.17E-03	7.23E-03	2.04E-03	0.013	3.252	Old
Acidaminococcus fermentans	Firmicutes	1.12E-04	6.96E-05	2.29E-04	3.51E-04	5.68E-03	9.68E-03	0.038	3.418	Old
Clostridium sp. CAG 609	Firmicutes	3.71E-04	2.08E-04	1.15E-04	4.87E-05	5.44E-05	2.99E-05	0.011	2.225	Young
Coprobacillus sp. CAG 826	Firmicutes	5.98E-04	1.67E-04	2.81E-04	1.05E-04	3.13E-04	2.74E-04	0.038	2.194	Young
Eubacterium sp. CAG 146	Firmicutes	1.78E-04	4.84E-05	1.93E-04	4.27E-05	4.93E-04	3.52E-04	0.027	2.169	Old
Eubacterium sp. CAG 180	Firmicutes	2.44E-03	1.04E-03	8.47E-04	5.44E-04	6.32E-04	4.63E-04	0.024	2.972	Young
Firmicutes bacterium CAG 536	Firmicutes	1.14E-04	3.48E-05	1.64E-04	4.38E-05	6.81E-04	4.71E-04	0.034	2.453	Old
Lactobacillus gasseri	Firmicutes	3.27E-04	3.31E-04	2.20E-05	2.05E-05	2.53E-04	3.60E-04	0.041	2.211	Young
Lactobacillus reuteri	Firmicutes	1.42E-02	9.52E-03	1.26E-03	1.09E-03	2.28E-02	2.81E-02	0.034	3.998	Old
Megasphaera cerevisiae	Firmicutes	5.33E-04	4.16E-04	2.97E-04	1.68E-04	1.21E-03	8.64E-04	0.046	2.633	Old
Megasphaera elsdenii	Firmicutes	1.82E-03	1.99E-03	1.99E-03	2.02E-03	1.16E-02	1.20E-02	0.029	3.664	Old
Megasphaera elsdenii CAG 570	Firmicutes	2.00E-04	1.99E-04	2.24E-04	2.19E-04	1.23E-03	1.26E-03	0.038	2.686	Old
Megasphaera sp. DJF-B143	Firmicutes	1.64E-04	6.49E-05	1.10E-04	3.26E-05	5.04E-04	4.56E-04	0.031	2.271	Old
Mitsuokella jalaludinii	Firmicutes	1.27E-04	4.85E-05	2.14E-04	2.06E-04	1.66E-03	1.57E-03	0.020	2.854	Old
Oscillibacter sp. CAG 155	Firmicutes	2.35E-03	4.04E-04	1.82E-03	6.16E-04	1.17E-03	1.78E-04	0.048	2.763	Young
Oscillibacter sp. CAG 241	Firmicutes	6.86E-03	1.65E-03	5.43E-03	3.69E-03	3.33E-03	9.12E-04	0.041	3.234	Young
Oscillibacter sp. KLE 1728	Firmicutes	5.26E-04	9.06E-05	4.01E-04	1.38E-04	2.89E-04	5.85E-05	0.034	2.071	Young
Oscillibacter valericigenes	Firmicutes	1.32E-03	2.94E-04	9.74E-04	4.08E-04	7.99E-04	1.70E-04	0.034	2.396	Young
Oscillospiraceae bacterium VE202-24	Firmicutes	9.14E-04	1.20E-04	6.76E-04	2.36E-04	4.59E-04	9.12E-05	0.024	2.348	Young
Roseburia sp. CAG 100	Firmicutes	9.12E-04	3.51E-04	1.48E-03	7.93E-04	5.80E-04	2.39E-04	0.034	2.672	Adult
Roseburia sp. CAG 309	Firmicutes	4.90E-04	2.39E-04	9.72E-04	3.34E-04	3.22E-04	2.96E-04	0.018	2.506	Adult
unclassified g Megasphaera	Firmicutes	2.04E-04	1.33E-04	1.45E-04	7.83E-05	8.10E-04	6.76E-04	0.027	2.499	Old
unclassified g Oscillibacter	Firmicutes	2.53E-03	4.62E-04	1.91E-03	6.65E-04	1.31E-03	2.70E-04	0.035	2.776	Young

(Continues)

TABLE A3 (Continued)

Species	Phylum	Relative abundance						p-value	LDA	Enrichment
		Young (mean)	Young (SD)	Adult (mean)	Adult (SD)	Old (mean)	Old (SD)			
Mannheimia succiniciproducens	Proteobacteria	2.48E-06	1.08E-06	2.98E-04	5.79E-04	7.25E-05	9.56E-05	0.019	2.126	Adult
Azonexus hydrophilus	Proteobacteria	8.67E-05	1.05E-04	1.44E-04	1.73E-04	1.53E-03	1.47E-03	0.024	2.839	Old
Azospira oryzae	Proteobacteria	1.90E-05	2.26E-05	3.02E-05	3.55E-05	3.34E-04	3.30E-04	0.024	2.179	Old
Azovibrio restrictus	Proteobacteria	4.35E-05	4.18E-05	6.33E-05	7.60E-05	6.64E-04	6.44E-04	0.028	2.472	Old
Dechloromonas agitata	Proteobacteria	1.22E-04	1.41E-04	2.01E-04	2.37E-04	2.12E-03	2.09E-03	0.024	2.979	Old
Dechloromonas aromatica	Proteobacteria	6.68E-05	7.96E-05	1.14E-04	1.37E-04	1.21E-03	1.18E-03	0.018	2.738	Old
Dechloromonas denitrificans	Proteobacteria	9.56E-05	1.15E-04	1.55E-04	1.88E-04	1.67E-03	1.66E-03	0.018	2.875	Old
Desulfovibrio desulfuricans	Proteobacteria	4.74E-05	2.22E-05	1.03E-04	5.25E-05	8.36E-04	1.41E-03	0.049	2.568	Old
Desulfovibrio fairfieldensis	Proteobacteria	4.56E-05	2.25E-05	1.22E-04	5.55E-05	9.50E-04	1.57E-03	0.018	2.631	Old
Desulfovibrio sp. 6-1-46AFAA	Proteobacteria	3.20E-05	1.47E-05	7.36E-05	3.55E-05	5.15E-04	8.26E-04	0.020	2.358	Old
Rhodocyclaceae bacterium Paddy-1	Proteobacteria	1.59E-05	1.85E-05	2.69E-05	3.25E-05	2.82E-04	2.70E-04	0.024	2.107	Old
Succinatimonas sp. CAG 777	Proteobacteria	1.18E-04	8.64E-05	5.14E-05	2.27E-05	7.80E-04	7.57E-04	0.043	2.561	Old

TABLE A4 The hosts of 39 differential bacteriophages based on the NCBI database

| Bacteriophage	Bacterial phylum	Bacterial species	Reference
Mycobacterium phage Courthouse	Actinobacteria	Mycobacterium smegmatis	https://www.ncbi.nlm.nih.gov/nuccore/NC_023690.1
Cellulophaga phage phi19-1	Bacteroidetes	Cellulophaga baltica	https://www.ncbi.nlm.nih.gov/nuccore/NC_021799.1
Cellulophaga phage phi10-1	Bacteroidetes	Cellulophaga baltica	https://www.ncbi.nlm.nih.gov/nuccore/NC_021802.1
Synechococcus phage S-SKS1	Cyanobacteria	Synechococcus sp. WH7803	https://www.ncbi.nlm.nih.gov/nuccore/NC_020851.1
Synechococcus phage ACG-2014d	NA	NA	https://www.ncbi.nlm.nih.gov/nuccore/NC_026923.1
Clostridium phage phiCP7R	Firmicutes	Clostridium perfringens	https://www.ncbi.nlm.nih.gov/nuccore/NC_017980.1
Enterococcus phage phiEF24C	Firmicutes	Enterococcus fecalis	https://www.ncbi.nlm.nih.gov/nuccore/NC_009904.1
Listeria phage P70	Firmicutes	Listeria sp.	https://www.ncbi.nlm.nih.gov/nuccore/NC_018831.1
Lactobacillus phage Ldl1	Firmicutes	Lactobacillus delbrueckii subsp. Lactis	https://www.ncbi.nlm.nih.gov/nuccore/NC_026609.1
Lactobacillus phage c5	Firmicutes	Lactobacillus delbrueckii subsp. bulgaricus	https://www.ncbi.nlm.nih.gov/nuccore/NC_019449.1
Staphylococcus phage S25-4	NA	NA	https://www.ncbi.nlm.nih.gov/nuccore/NC_022918.1
Staphylococcus phage 812	Firmicutes	Staphylococcus aureus	https://www.ncbi.nlm.nih.gov/nuccore/NC_029080.1
Staphylococcus phage GH15	Firmicutes	Staphylococcus aureus	https://www.ncbi.nlm.nih.gov/nuccore/NC_019448.1
Staphylococcus phage SAP-2	Firmicutes	Staphylococcus aureus	https://www.ncbi.nlm.nih.gov/nuccore/NC_009875.1
Lactococcus phage Tuc2009	Firmicutes	Lactococcus lactis	https://www.ncbi.nlm.nih.gov/nuccore/NC_002703.1
Streptococcus phage Dp-1	Firmicutes	Streptococcus pneumoniae	https://www.ncbi.nlm.nih.gov/nuccore/NC_015274.1
Streptococcus phage Str-PAP-1	Firmicutes	Streptococcus parauberis	https://www.ncbi.nlm.nih.gov/nuccore/NC_028666.1
Streptococcus phage phiNJ2	Firmicutes	Streptococcus suis NJ2 serotype 9	https://www.ncbi.nlm.nih.gov/nuccore/NC_019418.1
Aeromonas phage Aes012	Proteobacteria	Aeromonas sp.	https://www.ncbi.nlm.nih.gov/nuccore/NC_020879.1
Aeromonas phage 31	Proteobacteria	Aeromonas salmonicida	https://www.ncbi.nlm.nih.gov/nuccore/NC_007022.1
Campylobacter phage IBB35	NA	NA	https://www.ncbi.nlm.nih.gov/nuccore/NC_041833.1
Caulobacter phage CcrColossus	Proteobacteria	Caulobacter crescentus	https://www.ncbi.nlm.nih.gov/nuccore/NC_019406.1
Enterobacteria phage IME10	Proteobacteria	Escherichia coli	https://www.ncbi.nlm.nih.gov/nuccore/NC_019501.1
Salmonella phage SPN3US	NA	NA	https://www.ncbi.nlm.nih.gov/nuccore/NC_027402.1
Shigella phage Ag3	Proteobacteria	Shigella boydii	https://www.ncbi.nlm.nih.gov/nuccore/NC_013693.1
Enterobacteria phage phi92	Proteobacteria	Escherichia coli K92	https://www.ncbi.nlm.nih.gov/nuccore/NC_023693.1
Erwinia phage phiEaH2	Proteobacteria	Erwinia amylovora	https://www.ncbi.nlm.nih.gov/nuccore/NC_019929.1
Salmonella phage Stitch	Proteobacteria	Salmonella typhimurium	https://www.ncbi.nlm.nih.gov/nuccore/NC_027297.1
Escherichia phage Akfv33	Proteobacteria	Escherichia coli	https://www.ncbi.nlm.nih.gov/nuccore/NC_017969.1
Enterobacteria phage JSE	Proteobacteria	Escherichia coli K12	https://www.ncbi.nlm.nih.gov/nuccore/NC_012740.1
Yersinia phage phiR1 37	Proteobacteria	Yersinia enterocolitica.	https://www.ncbi.nlm.nih.gov/nuccore/NC_016163.1
Escherichia phage ECML-117	Proteobacteria	Escherichia coli	https://www.ncbi.nlm.nih.gov/nuccore/NC_025441.1
Pseudomonas phage EL	Proteobacteria	Pseudomonas aeruginosa	https://www.ncbi.nlm.nih.gov/nuccore/NC_007623.1
Sinorhizobium phage phiM9	Proteobacteria	Sinorhizobium meliloti	https://www.ncbi.nlm.nih.gov/nuccore/NC_028676.1
Vibrio phage VP882	Proteobacteria	Vibrio parahaemolyticus	https://www.ncbi.nlm.nih.gov/nuccore/NC_009016.1
Vibrio phage nt-1	Proteobacteria	Vibrio natriegens HER1138	https://www.ncbi.nlm.nih.gov/nuccore/NC_021529.2
Vibrio phage VPMS1	Proteobacteria	Vibrio parahaemolyticus Ex-1	https://www.ncbi.nlm.nih.gov/nuccore/NC_021776.1
Xylella phage Prado	Proteobacteria	Xylella fastidiosa	https://www.ncbi.nlm.nih.gov/nuccore/NC_022987.1
Halocynthia phage JM-2012	NA	NA	https://www.ncbi.nlm.nih.gov/nuccore/NC_017975.1
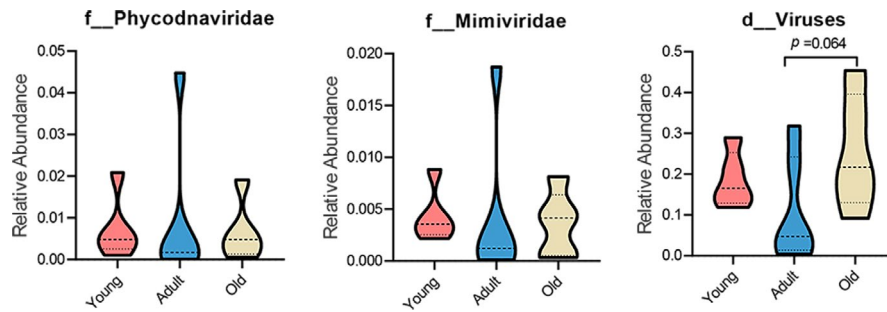
Figure A1 Quantification of the relative abundance of the three unassigned families. No significant difference was found among the three age groups. *p* values were determined by one-way ANOVA followed by LSD's multiple comparison tests. The following *n* values represented the number of independent animals for statistical evaluation: young, *n* = 5; adult, *n* = 6; and old, *n* = 5
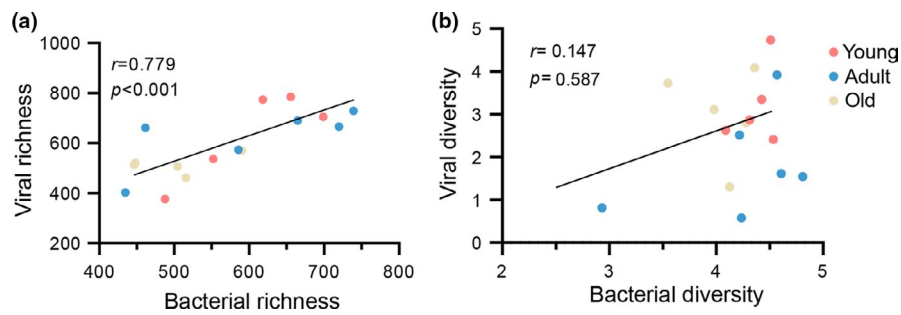

Figure A2 Positive relationships between the gut DNA viruses and bacteria. (a) Correlation plot between viral richness and bacterial richness. (b) Correlation between viral diversity and bacterial diversity. The lines indicate linear regression, and Spearman's correlation coefficient is shown. The color spectrum indicates age progression from young to old